Hydrodynamic disturbance on phosphorus release across the sediment–water interface in Xuanwu Lake, China

Yu Bai, Yuhong Zeng, Bei Nie, Helong Jiang and Xiaofeng Zhang

ABSTRACT

Excess phosphorus in lakes may cause algal blooming, and total phosphorus (TP) is an important index for lake eutrophication. As an important source of TP, lake sediment contributes a lot to TP release. TP release across the sediment–water interface varies with the hydrodynamic conditions of the overlying water, and in this paper the release characteristics of TP under hydrodynamic disturbance has been investigated. The sediment samples from Xuanwu Lake are collected and their release characteristics of TP under varying shear velocity are simulated in laboratory apparatus. Results show that increasing shear velocity contributes to the release of TP from sediment and the combination of varying shear velocity in different stages has a significant influence on the distribution of TP concentration. Further, the lattice Boltzmann method (LBM) is used to simulate the process of TP release from the sediment–water interface and the predicted values agree well with the measured data, which proves that the LBM can be used in simulating the process of TP release from sediment.

Key words | eutrophication, hydrodynamic disturbance, lattice Boltzmann method, phosphorus release, shear velocity

Yu Bai
Yuhong Zeng (corresponding author)
Bei Nie
Xiaofeng Zhang
School of Water Resources and Hydropower Engineering,
Wuhan University,
Wuhan 430072,
China
E-mail: *yhzeng@whu.edu.cn*

Helong Jiang
State Key Laboratory of Lake Science and Environment,
Nanjing Institute of Geography and Limnology,
Chinese Academy of Sciences,
Nanjing 210008,
China

INTRODUCTION

The impact of total phosphorus (TP) on the shallow lake environment has been in the focus of environmental engineering in recent years. TP plays an essential role in the growth of plants, while excess TP can have significant detrimental effects on water environments, one of which is to cause algal blooms. Except for that released by waste water from industry and urban areas, the sediment is also an important source for TP in shallow lakes. In recent years, sludge dredging has become an important measure for water environment restoration in lakes and rivers, for its high efficiency (Liu *et al.* 2016; Wang *et al.* 2016; Zhao *et al.* 2017). But dredging projects will disturb the TP in the sediment and may cause serious effects on the water environment especially for those shallow lakes.

In the past decades, a variety of laboratory models have been applied to study the release characteristics of TP across the sediment–water interface under hydrodynamic disturbance (Huang *et al.* 2015). The release process of TP can be described by three stages: the rapid release stage, slow release stage, and stable release stage. In the initial release stage, the vertical distribution of TP along the overlying water is not uniform, and the release rate of TP under hydrodynamic disturbance can be six times higher than that under hydrostatic conditions (Zhang *et al.* 2012). Huang *et al.* (2016) conducted experiments in a round container, and a propeller rotating with the motor to simulate different hydrodynamic conditions. They found that the TP release rate decreased with increasing the propeller speed from 300 rad min^{-1} to 400 rad min^{-1}, and concluded that low to moderate hydrodynamic disturbance can promote the release of TP. The effect of vegetation on the release of TP was also taken into account by Wu & Hua (2014), and the shear velocity at the sediment–water interface was simulated by varying wind velocity above the water surface. Their results show that vegetation has a significant effect on decreasing the release of TP, especially in disturbed conditions induced by stable and rapid wind. TP release in an annular flume has also

doi: 10.2166/ws.2018.115

been investigated, and typically a motor located in the middle of the flume drives a propeller to simulate different hydrodynamic conditions. Results show that the release rate of phosphorus (P) in flume bed sediment is also accelerated with the increase of shear velocity (Couceiro *et al.* 2013).

The lattice Boltzmann method (LBM) has been widely applied to solve the diffusion problem, as it has advantages in simulating a complex physical system and dealing with a complex physical boundary compared with other traditional methods (finite volume method, finite difference method and finite element method etc.). Wissocq *et al.* (2017) adopt LBM to simulate high Reynolds number flow by testing and implementing three different characteristic boundary conditions with open source LBM code. A revised LBM is proposed by Hu *et al.* (2016) to simulate the convection diffusion equation with multi-relaxation time, and the result proves that it is suitable for simulating both isotopic and anisotropic diffusion processes. The lake sediment is a porous medium, and they prove that the LBM is effective in simulating porous media with uniform and non-uniform porosity (Chen *et al.* 2017).

Although lots of studies have been done in the past, most of them only considered the constant shear velocity on the TP release (Zhu *et al.* 2013; Wang *et al.* 2015). While the hydrodynamic condition of lakes is changeable and its effect on release of TP in different stages may be different, so the varying hydraulic disturbance on TP release from the sediment still needs further investigation. In this paper, we consider the dynamic varying of the water current in the experiments by adopting a three-stage shearing velocity which is closer to the real condition of the lake. Further, the LBM is used to simulate the release of TP from the interface between overlying water and sediment.

MATERIALS AND METHODS

Study area and sampling

Xuanwu Lake (32°4′N, 118°47′E) is an urban shallow lake located in the northeast of Nanjing, China. As one of the five biggest urban lakes in China, Xuanwu Lake has a history of 1,500 years. It has three parts (North Lake, Southwest Lake and Southeast Lake), with surface area 3.7 km^2, average depth of 1.14 m, and highest water level of 2.31 m. Due to the increasing population, large amounts of waste water have been discharged into the lake, and the water quality is worsening. A Petersen grab sampler was used to collect the surface sediment (0–10 cm depth) in Xuanwu Lake on 10 March 2017, and the sample site (site 32°4′1″N, 118°47′34″E) is shown in Figure 1(a). The grain diameter characteristics of the sediment, measured by laser particle size analyzer, are shown in Table 1.

Experimental parameters

The laboratory experiment (as shown in Figure 1(b)) was conducted in a round Plexiglas container with a diameter of 30 cm and height of 50 cm. A motor was mounted above the container and its rotating velocity was changeable to produce varying shear velocity on the sediment surface. Because there were lots of impurities such as snails, the sediment was sieved before the experiment. At the beginning of the experiments, the sediment was fully stirred and its thickness was kept as 10 cm; 20 L deionized water was slowly added into the container, and then it was left undisturbed for 24 h before the experiment.

Each experimental period (9 hours) was divided into three stages (the first 3 hours, the middle 3 hours, and the last 3 hours), and three rotating speeds of the propeller, 100 rad min^{-1}, 200 rad min^{-1} and 300 rad min^{-1} were adopted. Run EX1 was also conducted as a control run. In total seven runs were conducted, and the corresponding rotating speeds of the propeller are listed in Table 2. During the experiment, we sampled three water samples simultaneously every 1 h, as each sample was 100 ml. The

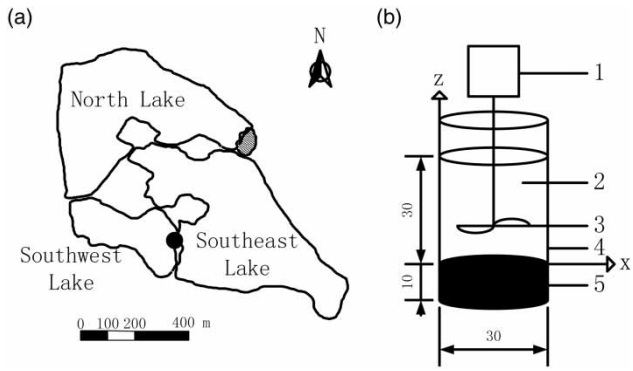

Figure 1 | (a) Location of sampling in Xuanwu Lake; (b) sketch of the model (cm): 1. motor; 2. overlying water; 3. propeller; 4. Plexiglas cylinder; 5. sediment.

Table 1 | Grain diameter distribution of the sediment

Grain diameter (D, μm)	Percentage (%)
$D<4$	13.14
$4<D<16$	28.8
$16<D<32$	19.71
$32<D<64$	19.54
$64<D<128$	12.44
$D>128$	6.37

Table 2 | Experimental parameters

Run	First stage (rad min^{-1})	Second stage (rad min^{-1})	Third stage (rad min^{-1})
EX1	0	0	0
EX2	100	100	100
EX3	200	200	200
EX4	300	300	300
EX5	100	200	300
EX6	200	300	100
EX7	300	100	200

samples were centrifuged, then, and TP was determined by Mo-Sb anti-spectrophotometry method. The sediment was sampled at 0 h, 1 h, 3 h, 5 h, 7 h, and 9 h, and the sampled sediment was dried, crushed, sieved and digested.

Lattice Boltzmann method

Governing equations

Nutrient release in lakes includes that from sediment and diffuse in the overlying water; and for sediment release, there is a diffusion process, and adsorption and desorption process. The diffusion rate can be measured by the nutrient concentration gradient in the pore water of the sediment with Fick's first law, and the adsorption and desorption can be defined by a source item (Higashino & Stefan 2011; Inoue & Nakamura 2012).

The nutrient release from sediment can be expressed as follows:

$$\varphi\frac{\partial C}{\partial t}=\varphi D_{zs}\frac{\partial^2 C}{\partial z^2}-\rho_b\frac{\partial c_s}{\partial t}\,(\text{for}\,z<0), \tag{1}$$

where c is the nutrient concentration in water (mg l^{-1}, a litre is equal to 10^{-3} cubic metres); t is time (s); φ is the porosity of sediment; z is the vertical axis originated (at the sediment–water interface $z=0$); D_{zs} is the diffusion coefficient of nutrient in sediment (m^2 s^{-1}); $\rho_b(\partial c_s/\partial t)$ is a source term for nutrient adsorption and desorption (Wang 2008); c_s is the quantity of nutrient adsorption (mg kg^{-1}); ρ_b is the density of sediment (kg m^{-3}).

The Lagergren first-order (LFO) equation is commonly used for describing the adsorption and desorption, and it is well suited for explaining adsorption and desorption kinetics (Tseng *et al.* 2010):

$$\frac{\partial c_s}{\partial t}=b(c_{se}-c_s), \tag{2}$$

where b is the first-order rate constant (s^{-1}); c_{se} is the sediment contamination level (mg kg^{-1}).

Yuan *et al.* (2017) assume that the amount of desorption of sediment samples is equal to the amount added to the solutions. Then, they modified the LFO equation as (Yuan *et al.* 2017):

$$\frac{\partial c}{\partial t}=b(c_e-c), \tag{3}$$

where c_e is the equilibrium concentration of TP in water (mg l^{-1}). If $c>c_e$, the sediment adsorbs TP from the water. When $c<c_e$, TP releases from the sediment to the water; a large gap between c and c_e means a high adsorption or desorption rate (Zhang *et al.* 2014; Yin *et al.* 2016).

The modified LFO model only considers constant hydrodynamic conditions and it shows that c_e is unchanged in constant conditions, so in an airtight container without TP input, the concentration of TP in the overlying water and sediment would have a constant value. But under the action of shear velocity, c_e will vary with the change of hydrodynamic conditions (or the adsorption rate decreases and c_e increases with the increasing shear velocity (Li *et al.* 2016)).

Here we modified the second term on the right of Equation (1) as:

$$\rho_b\frac{\partial c_s}{\partial t}=b(c-c_e), \tag{4}$$

when $c > c_e$, $b(c - c_e)$ is positive indicating adsorption; when $c < c_e$, $b(c - c_e)$ is negative indicating release. As c_e varies with the hydrodynamic conditions of the overlying water, we introduced a coefficient a to describe the effect of hydraulic disturbance on c_e, and Equation (4) is written as:

$$\rho_b \frac{\partial c_s}{\partial t} = b(c - ac_{e0}), \tag{5}$$

where a is a coefficient related to shear velocity (a and b can be determined by experiment and a is equal to 1 under static hydrodynamic conditions); c_{e0} is the equilibrium concentration of TP in water under static hydrodynamic conditions (mg l^{-1}).

D_{zs} can be expressed as:

$$D_{zs} = \varphi^{m-1} D_{zm}, \tag{6}$$

where D_{zm} is the molecular diffusion coefficient in water ($m^2\ s^{-1}$), which varies with the targeting solution; $m = 3$ is a constant (Ullman & Aller 1982).

In the overlying water, the formulations can be simply described as the diffusion process and the biochemical reactions are assumed to be negligible. The governing equations can be expressed as (Inoue & Nakamura 2010):

$$\frac{\partial C}{\partial t} = (D_{zt} + D_{zm}) \frac{\partial^2 C}{\partial z^2} (\text{for } z \geq 0), \tag{7}$$

$$\frac{D_{zt}}{v} = \left(A \frac{z u_*}{v}\right)^n, \tag{8}$$

where D_{zt} is turbulent diffusion coefficient ($m^2\ s^{-1}$), A is the area of water–sediment interface (m^2), v is the kinematic viscosity of water ($m^2\ s^{-1}$), and $n = 3$ is a constant (van Rijn 1984); u_* is the shear velocity, and that generated by the propeller is given by Chandler (2012):

$$u_* = 8.67 \times 10^{-5} \text{ (propeller speed)} - 3.27 \times 10^{-3}. \tag{9}$$

LBM for TP release

A two-dimensional (D2Q4) model is adopted and the LBM equation can be obtained by temporally and spatially discretizing. The governing functions of the LBM model in overlying water and sediment are given in Table 3. The difference between overlying water and sediment in the LBM are the evolution equation and relaxation frequency functions.

Boundary conditions

By applying the LBM, the free surface of the overlying water can be defined as a thermal insulating boundary. The nutrient concentration gradient of the free surface is 0,

$$\frac{\partial c}{\partial z} = 0. \tag{10}$$

The container wall is defined as a rebound boundary.

Table 3 | Governing functions of sediment and overlying water[a]

Function	Overlying water	Sediment
Transport	$f_k(x + \Delta x, z + \Delta z, t + \Delta t) = f_k(x, z, t + \Delta t)$	
Evolution	$f_k(x, z, t + \Delta t) = f_k(x, z, t)(1 - \omega) + \omega f_k^{eq}(x, z, t)$	$f_k(x, z, t + \Delta t) = f_k(x, z, t)(1 - \omega) + \omega f_k^{eq}(x, z, t) - \Delta t w_k b(c(x, z, t) - ac_{e0})$
Relaxation frequency	$\omega = 1/\left(\frac{2\Delta t(D_{zt} + D_{zm})}{\Delta x^2} + 0.5\right)$	$\omega = 1/\left(\frac{2\Delta t D_{zs}}{\Delta x^2} + 0.5\right)$
Equilibrium distribution	$f_k^{eq}(x, z, t) = w_k c(x, z, t)$	
Distribution	$c(x, z, t) = \sum_{k=1}^{4} f_k(x, z, t)$	

[a]Δt is time step; ω is relaxation frequency; f_k is the particle distribution function in terms of a discrete particle in direction k; f_k^{eq} is the equilibrium distribution function in direction k; $w_1 = w_2 = w_3 = w_4 = 0.25$.

EXPERIMENTAL RESULTS AND DISCUSSION

Effect of shear velocity on TP release from the sediment

For static conditions (EX1), TP concentration reduced during the experiment, indicating the adsorption of TP by the sediment (Figure 2). For hydrodynamic condition experiments, TP concentrations of EX2, EX3 and EX4 ranged from $0.0473\ \mathrm{mg\,l^{-1}}$ to $0.0771\ \mathrm{mg\,l^{-1}}$, $0.0546\ \mathrm{mg\,l^{-1}}$ to $0.1432\ \mathrm{mg\,l^{-1}}$ and $0.0611\ \mathrm{mg\,l^{-1}}$ to $0.1663\ \mathrm{mg\,l^{-1}}$, respectively for the 9 experimental hours. As deionized water was used as the overlying water, its TP concentration was much lower than that in Xuanwu Lake (TP concentration ranged from 1.43 to $2.6\ \mathrm{mg\,l^{-1}}$). TP concentration in the water increased quickly in the early 3 hours, then slowed down in the mid 3 hours and remained substantially unchanged in the last 3 hours. TP concentration increased with increasing shear velocity and the TP concentration of EX5 was higher than the others. A good correlation between the shear velocity and TP concentration was proved by a variance test, and all the release processes can be fitted by a logarithmic curve.

The effect of combinations of shear velocity on TP concentration

In EX5, TP release rate was small in the first stage, then increased in the last two stages and the total release amount of TP was higher than in EX6 and EX7 (Figure 3). In EX6, the release rate in the first stage was higher than in EX5, then the release rate increased slowly in the second stage and in the last stage it had an obvious downward trend. The total release amount of TP was less than EX5 and EX7. In EX7, TP release rate was highest in the first stage. It had a downward trend in the second stage and increased a little in the last stage. This proved that gradual increase of rotation speed was conducive to TP release and the abrupt decrease of rotation speed will cause a decline of TP concentration in the last two stages. The effect of varying shear velocity on TP release cannot be calculated by simple addition, since different shear velocity at different stages has an interactive influence on the release amount of TP.

MODEL VERIFICATION

Time step was set to 1 s ($\Delta t = 1$ s). The free surface of the overlying water was defined as a thermal insulating boundary, and the Plexiglas wall was defined as a rebound boundary. When $-10\ \mathrm{cm} < z < 0\ \mathrm{cm}$, TP release occurs; when $0\ \mathrm{cm} \le z \le 30\ \mathrm{cm}$, TP diffusion occurs. Before simulation, we needed to determine the parameters a and b, which are related to the shear velocity, firstly. EX1, EX2, EX3 and EX4 were used as calibration data and the remaining data as validation data. The parameter a was determined by combining the LBM with an optimization algorithm. The

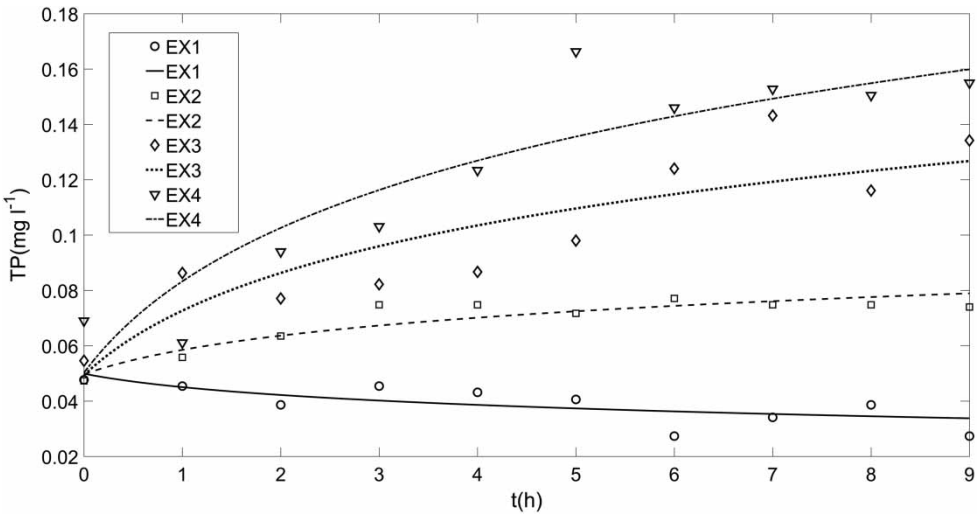

Figure 2 | Variations of TP concentration in overlying water with time.

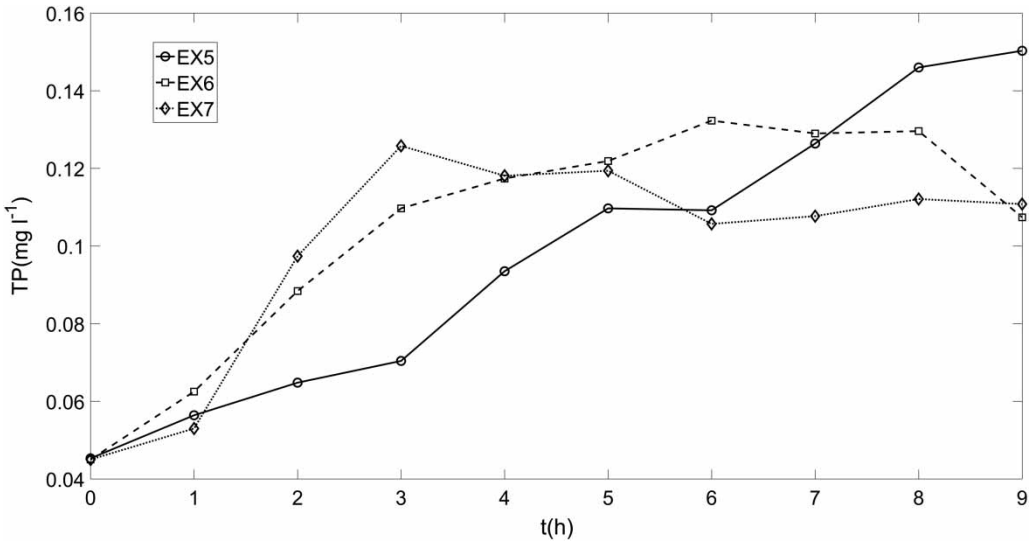

Figure 3 | Variations of TP release rate with different shear velocities.

objective function of the optimization algorithm was as follows,

$$fx = \sum_{i=1}^{p} (\hat{y}_i - y_i)^2, \tag{11}$$

where $\hat{y}_i$ is the predicted value of TP concentration by the LBM; y_i is the measured value of TP concentration; p is the group of calibrated data, here $p = 4$; fx is the variance between the measured and predicted value.

The program was run until the global optimal solution was determined, and finally we got the determination coefficient (R^2) of the predicted values and the measured values of EX1 to EX4, which are higher than 0.99. The root mean square (RMS) of the predicted values and the measured values of EX1 to EX4 are lower than 0.005. The parameter b is 0.3 and the parameter a can be synthesized in the following form:

$$a = -4627.8u_*^2 + 290.88u_* + 1, \tag{12}$$

Table 4 | Comparison between predicted data and measured data: TP concentration

Experiment		1 h	2 h	3 h	4 h	5 h	6 h	7 h	8 h	9 h	R^2	RMS
1	Measured Value	0.045	0.042	0.04	0.039	0.037	0.036	0.035	0.035	0.034	0.991	0.0023
	Predicted Value	0.051	0.046	0.042	0.039	0.037	0.036	0.035	0.034	0.034		
2	Measured Value	0.059	0.064	0.067	0.07	0.073	0.074	0.076	0.078	0.079	0.99	0.0012
	Predicted Value	0.056	0.063	0.067	0.071	0.073	0.075	0.076	0.077	0.078		
3	Measured Value	0.073	0.086	0.096	0.104	0.11	0.115	0.119	0.123	0.127	0.99	0.0045
	Predicted Value	0.061	0.081	0.095	0.105	0.112	0.117	0.12	0.123	0.124		
4	Measured Value	0.083	0.103	0.116	0.127	0.136	0.143	0.149	0.155	0.16	0.99	0.0071
	Predicted Value	0.065	0.093	0.114	0.129	0.139	0.146	0.151	0.155	0.157		
5	Measured Value	0.056	0.065	0.070	0.094	0.11	0.109	0.126	0.146	0.15	0.987	0.0119
	Predicted Value	0.056	0.063	0.067	0.076	0.091	0.103	0.114	0.128	0.139		
6	Measured Value	0.063	0.088	0.11	0.117	0.122	0.132	0.129	0.13	0.107	0.96	0.0076
	Predicted Value	0.061	0.081	0.095	0.109	0.125	0.136	0.135	0.119	0.107		
7	Measured Value	0.053	0.097	0.126	0.118	0.119	0.106	0.108	0.112	0.111	0.955	0.0079
	Predicted Value	0.065	0.093	0.114	0.12	0.109	0.1	0.099	0.107	0.113		

and a ranged from 1 to 5.25 when u_* varied from 0 to 0.0227 m s^{-1}. The validation result shows that R^2 of EX5, EX6 and EX7 (validation data) are 0.987, 0.96 and 0.955 (Table 4). The R^2 of all measured and predicted values is higher than 0.951, and the RMS of all measured and predicted values is lower than 0.012. Most of the simulated values are smaller than the experimental values.

CONCLUSIONS

Laboratory experiments have been conducted to simulate the TP release process and evaluate the release rate across the sediment–water interface. During TP release, there are diffusion, adsorption and desorption processes. By considering the variation of adsorption and desorption items with the effect of hydraulic disturbance in the controlling equations, the release process of TP from the sediment was numerically predicted using the LBM.

Results show that the TP release rate increased with the increase of shear velocity and the release process can be fitted well to a logarithmic function. For static conditions, desorption was dominant and the nutrient release rate was negative. The increase of shear velocity had a positive effect on the release of TP and the sudden decrease of shear velocity decreased the release rate of TP. Here only low initial TP concentration conditions have been tested and our findings are valid for those without TP input conditions. In conditions with TP input or higher initial TP concentration conditions, the source item of TP adsorption and desorption may be different.

ACKNOWLEDGEMENTS

This work was supported in part by the National Research and Development Program of China (No. 2016YFA0600901), Hubei Natural Science Foundation (2018CFA010), CAS Interdisciplinary Innovation Team, and 111 Project (B18037).

REFERENCES

Chandler, I. D. 2012 *Vertical Variation in Diffusion Coefficient within Sediments*. Doctoral dissertation, University of Warwick, UK.

Chen, S., Yang, B. & Zheng, C. 2017 Simulation of double diffusive convection in fluid-saturated porous media by lattice Boltzmann method. *International Journal of Heat and Mass Transfer* **108**, 1501–1510.

Couceiro, F., Fones, G. R., Thompson, C. E. L., Statham, P. J., Sivyer, D. B., Parker, R., Kelly-Gerreyn, B. A. & Amos, C. L. 2013 Impact of resuspension of cohesive sediments at the Oyster Grounds (North Sea) on nutrient exchange across the sediment–water interface. *Biogeochemistry* **113** (1–3), 37–52.

Higashino, M. & Stefan, H. G. 2011 Non-linear effects on solute transfer between flowing water and a sediment bed. *Water Research* **45** (18), 6074–6086.

Hu, Y., Li, D., Shu, S. & Niu, X. 2016 Lattice Boltzmann flux scheme for the convection–diffusion equation and its applications. *Computers & Mathematics with Applications* **72** (1), 48–63.

Huang, J., Xu, Q., Xi, B., Wang, X., Li, W., Gao, G., Huo, S., Xia, X., Jiang, T., Ji, D., Liu, H. & Jia, K. 2015 Impacts of hydrodynamic disturbance on sediment resuspension, phosphorus and phosphatase release, and cyanobacterial growth in Lake Tai. *Environmental Earth Sciences* **74** (5), 3945–3954.

Huang, J., Xi, B. D., Xu, Q. J., Wang, X. X., Li, W. P., He, L. S. & Liu, H. L. 2016 Experiment study of the effects of hydrodynamic disturbance on the interaction between the cyanobacterial growth and the nutrients. *Journal of Hydrodynamics, Ser. B* **28** (3), 411–422.

Inoue, T. & Nakamura, Y. 2010 Effects of hydrodynamic conditions on DO transfer at a rough sediment surface. *Journal of Environmental Engineering* **137** (1), 28–37.

Inoue, T. & Nakamura, Y. 2012 Response of benthic soluble reactive phosphorus transfer rates to step changes in flow velocity. *Journal of Soils and Sediments* **12** (10), 1559–1567.

Li, Z., Tang, H., Xiao, Y., Zhao, H., Li, Q. & Ji, F. 2016 Factors influencing phosphorus adsorption onto sediment in a dynamic environment. *Journal of Hydro-Environment Research* **10**, 1–11.

Liu, C., Zhong, J., Wang, J., Zhang, L. & Fan, C. 2016 Fifteen-year study of environmental dredging effect on variation of nitrogen and phosphorus exchange across the sediment-water interface of an urban lake. *Environmental Pollution* **219**, 639–648.

Tseng, R. L., Wu, F. C. & Juang, R. S. 2010 Characteristics and applications of the Lagergren's first-order equation for adsorption kinetics. *Journal of the Taiwan Institute of Chemical Engineers* **41** (6), 661–669.

Ullman, W. J. & Aller, R. C. 1982 Diffusion coefficients in nearshore marine sediments. *Limnology and Oceanography* **27** (3), 552–556.

van Rijn, L. C. 1984 Sediment transport, part III: bed forms and alluvial roughness. *Journal of Hydraulic Engineering* **110** (12), 1733–1754.

Wang, H. T. 2008 *Dynamics of Fluid Flow and Contaminant Transport in Porous Media*. Higher Education Press, Beijing, China, pp. 36–37.

Wang, J., Pang, Y., Li, Y., Huang, Y. & Luo, J. 2015 Experimental study of wind-induced sediment suspension and nutrient release in Meiliang Bay of Lake Taihu, China. *Environmental Science and Pollution Research* **22** (14), 10471–10479.

Wang, C., Bai, L., Jiang, H. L. & Xu, H. 2016 Algal bloom sedimentation induces variable control of lake eutrophication by phosphorus inactivating agents. *Science of the Total Environment* **557–558**, 479–488.

Wissocq, G., Gourdain, N., Malaspinas, O. & Eyssartier, A. 2017 Regularized characteristic boundary conditions for the Lattice-Boltzmann methods at high Reynolds number flows. *Journal of Computational Physics* **331**, 1–18.

Wu, D. & Hua, Z. 2014 The effect of vegetation on sediment resuspension and phosphorus release under hydrodynamic disturbance in shallow lakes. *Ecological Engineering* **69**, 55–62.

Yin, H., Han, M. & Tang, W. 2016 Phosphorus sorption and supply from eutrophic lake sediment amended with thermally-treated calcium-rich attapulgite and a safety evaluation. *Chemical Engineering Journal* **285**, 671–678.

Yuan, L., Han, L., Bo, W., Chen, H., Gao, W. & Chen, B. 2017 Simulated oil release from oil-contaminated marine sediment in the Bohai Sea, China. *Marine Pollution Bulletin* **118** (1–2), 79–84.

Zhang, K., Cheng, P. D., Zhong, B. C. & Wang, D. Z. 2012 Total phosphorus release from bottom sediments in flowing water. *Journal of Hydrodynamics, Ser. B* **24** (4), 589–594.

Zhang, Y., He, F., Xia, S., Kong, L., Xu, D. & Wu, Z. 2014 Adsorption of sediment phosphorus by porous ceramic filter media coated with nano-titanium dioxide film. *Ecological Engineering* **64**, 186–192.

Zhao, S., Shi, X., Li, C., Zhang, S., Sun, B., Wu, Y. & Zhao, S. 2017 Diffusion flux of phosphorus nutrients at the sediment–water interface of the Ulansuhai Lake in northern China. *Water Science and Technology* **75** (6), 1455–1465.

Zhu, H. W., Cheng, P. D., Zhong, B. C. & Wang, D. Z. 2013 Hydrodynamic effects on contaminants release due to resuspension and diffusion from sediments. *Journal of Hydrodynamics, Ser. B* **25** (5), 731–736.

First received 4 March 2018; accepted in revised form 11 June 2018. Available online 19 June 2018